ISSN 1392 - 1207. MECHANIKA. 2010. Nr.3(83)

Effect of sensor locations on the solution of inverse Stefan problems

A. Abbas Nejad*, M.J. Maghrebi, H. Basirat Tabrizi*****

**Mechanical Engineering Department, Shahrood University of Technology, P.O. 3619995161 Shahrood, Iran, E-mail: abbasnejad@shahroodut.ac.ir*

***Mechanical Engineering Department, Shahrood University of Technology, P.O. 3619995161 Shahrood, Iran, E-mail: javad@shahroodut.ac.ir*

****Faculty of Mechanical Engineering, Amirkabir University of Technology, Tehran, Iran, E-mail: hbasirat@aut.ac.ir*

1. Introduction

Inverse Heat Conduction Problem (IHCP) has received a special attention from engineers, mathematicians and physicists[1]. It has many applications in different branches of science and technology. One of the most important applications of IHCP is solidification processes, because the quality of solidified material is deeply dependent on the cooling boundary conditions [2]. So the cooling rate at the boundary and thus the solid-liquid interface velocity define the solidified materials quality. Thus, the desired material structures with desired quality and mechanical properties can be obtained by controlling the thermal boundary conditions.

A wide variety of numerical methods were used for direct and inverse modelling of solidification problems. Voller [3] presented an enthalpy method with future time stepping to solve inverse Stefan problem. The problem was investigated with and without fluid flow consideration using Beck's method, the steepest descent method and conjugate gradient method by references [4-11]. They used front fixing and front tracking finite element method. In their approach the problem should be treated as two distinct inverse problems for both liquid and solid phases. Frankel and Keyhani [12] and Hale et. al. [13] applied the global time method (GTM) to control interfacial temperature gradient and velocity. Xu and Naterer [14-16] estimated boundary temperature history to control the velocity and acceleration of the interface using combined experimental and numerical techniques. The numerical method was developed for enthalpy with control volume based finite element method and Beck's inverse method. Recently, Okamoto and Li [17] used Tikhonov regularization method to control the velocity and the shape of the solid-liquid interface. Hinze and Ziegenbaly [18] solved inverse Stefan problem for one and two region problems using steepest descent method.

In this study, the heat flux test case is applied as a boundary condition and the temperatures at different sensor locations are recorded. These temperatures are used as desired temperatures or measured temperatures. Then the objective of the IHCP is to reconstruct a boundary heat flux which leads to this temperature history at sensor locations. The cost functional is defined based on temperature difference between the desired temperature and the computed temperature at the sensor location. The accuracy of the solution can be evaluated in comparison of the results with the first input heat flux, used to generate desired temperatures. The effect of different sensor locations is investigated on the solution of inverse problem. The results show that the solution is less accurate especially when the sensor is far from the active boundary. A random noise is added to the measured temperatures to evaluate the efficiency of solution under the perturbed input data in real practical measurements due to the instruments error. The simulated results show a close agreement with desired one even in high noise levels.

2. Governing equations

The unidirectional conduction-dominated solidification of a pure material with boundary conditions is shown in Fig. 1. The governing equations of the problem in enthalpy form are nondimensioned as equations set (1) using following nondimensional distance, time, temperature, enthalpy, Stefan number and boundary heat flux

$$\bar{x} = \frac{x}{a},\ \bar{t} = \frac{\alpha t}{a^2},\ \bar{T} = \frac{T - T_f}{T_f - T_0},\ \bar{H} = \frac{H}{C_p(T_f - T_0)},$$

$$Ste = \frac{L}{C_p(T_f - T_0)},\ \bar{q} = \frac{q(t)a}{k(T_f - T_0)}$$

where H is the enthalpy, T is the temperature and $q(t)$ is the boundary heat flux, *Ste* is the nondimensional form of latent heat known as Stefan's number.

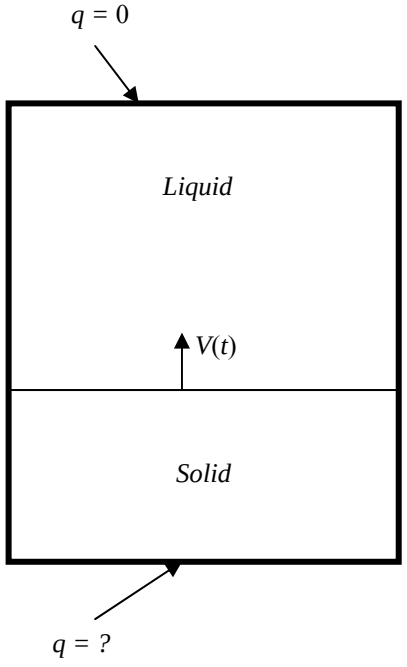

Fig. 1 Schematic problem representation

Thus, the nondimensional model equations describing the temperature distribution in the solidifying region based on enthalpy form can be written as follows [19]. The sign over the nondimensional parameters is neglected for simplicity.

$$\left.\begin{aligned} &\frac{\partial H}{\partial t}=\frac{\partial^2 T}{\partial x^2}, \quad 0<x<1, \quad 0<t\le t_f \\ &\left.\frac{\partial T}{\partial x}\right|_{x=0}=q(t), \quad x=0, \quad 0<t\le t_f \\ &\left.\frac{\partial T}{\partial x}\right|_{x=1}=q(t), \quad x=1, \quad 0<t\le t_f \\ &T=T_i \ or \ H=H_i, \quad 0\le x\le 1, \quad t=0 \end{aligned}\right\} \tag{1}$$

The enthalpy-temperature relations are

$$\left.\begin{aligned} H(x,t)&=\begin{cases} T & T<0 \quad Solid\ region \\ [0, Ste] & T=0 \\ T+Ste & T>0 \quad Liquid\ region \end{cases} \\ T(x,t)&=\begin{cases} H & H<0 \quad Solid\ region \\ 0 & 0\le H\le Ste \quad Interface \\ H-Ste & H>Ste \quad Liquid\ region \end{cases} \end{aligned}\right\} \tag{2}$$

The direct problem given by the sets of Eqs. (1) and (2) is for the determination of the temperature field $T(x,t)$ and the interface velocity when the boundary heat flux $q(t)$ at $x=0$ is known.

On the other hand for the inverse problem, the heat flux $q(t)$ at $x=0$ is unknown while the temperatures at some points, velocity, acceleration or location of interface are known. The heat flux can be estimated by using the measured temperatures or the desired temperatures (pseudo measured temperatures).

So the inverse problem is established which minimizes the objective function, cost function, defined base on the L_2 norm of the error between the calculated and the desired temperatures at sensor location (xm: measurement point). In other words[1, 20]

$$\begin{aligned} s[q(t)] &= \| T_t - T(x_{sd}, t; q(t)) \|^2 = \\ &= \int_0^{t_f} [T_f - T(x_{sd}, t; q(t))]^2 dt \end{aligned} \tag{3}$$

The conjugate gradient method with adjoint problem is applied to minimize the cost function of Eq. (3).

3. The sensitivity problem

It is assumed that the temperature $T(x,t)$ and the enthalpy $H(x,t)$ change with an amount $\Delta T(x,t)$ and $\Delta H(x,t)$, respectively when $q(t)$ undergoes a perturbation $\Delta q(t)$. By substituting $[T+\Delta T]$ for $T(x,t)$, $[H+\Delta H]$ for $H(x,t)$ and $[q+\Delta q]$ for $q(t)$ in the direct problem Eq. (1) and subtracting the original direct problem the following expressions are obtained as introduced in [20]

$$\left.\begin{aligned} &\frac{\partial \Delta H}{\partial t}=\frac{\partial^2 \Delta T}{\partial x^2}, \quad 0<x<1, \quad 0<t\le t_f \\ &\frac{\partial \Delta T}{\partial x}=\Delta q, \quad x=0, \quad 0<t\le t_f \\ &\frac{\partial \Delta T}{\partial x}=0, \quad x=1, \quad 0<t\le t_f \\ &\Delta T=0, \quad 0\le x\le 1, \quad t=0 \end{aligned}\right\} \tag{4}$$

As $\Delta H=\Delta T$. Clearly $\Delta T(x,t)$ represents changes in $T(x,t)$ with respect to the changes in the unknown $q(t)$; hence, is a sensitivity function. Eqs. (4) can be solved to obtain an optimal search step size.

4. The adjoint problem

To derive the adjoint problem, a new function $\lambda(x,t)$ called Lagrange multiplier is introduced. In adjoint problem the governing equations are multiplied by $\lambda(x,t)$ and integrated over the spatial and temporal domains. The results are then added to the cost functional Eq. (3) as achieved in [20]

$$\begin{aligned} s[q(t)] = &\int_0^{t_f} [T_f - T(x_m, t; q(t))]^2 dt + \\ &\int_0^{t_f}\int_0^1 \lambda(x,t)[k\frac{\partial^2 T}{\partial x^2} - \rho\frac{\partial H}{\partial t}]dxdt \end{aligned} \tag{5}$$

The following adjoint problem can be obtained by replacing T by $[T+\Delta T]$, q by $[q+\Delta q]$ and $s(q)$ by $[s(q)+\Delta s(q)]$ in Eq. (5) then subtracting the obtained result from Eq. (5) and further using boundary and initial conditions and allowing terms containing $\Delta T(x,t)$ to vanish

$$\left.\begin{aligned} &\frac{\partial \lambda(x,t)}{\partial t}+\frac{\partial^2 \lambda(x,t)}{\partial x^2}+ \\ &+2[T-T_f]\delta(x-x_{sd})=0, \quad 0<x<1, \quad 0<t\le t_f \\ &\frac{\partial \lambda}{\partial x}=0, \quad x=0, \quad 0<t\le t_f \\ &\frac{\partial \lambda}{\partial x}=0, \quad x=1, \quad 0<t\le t_f \\ &\lambda=0, \quad 0\le x\le 1, \quad t=t_f \end{aligned}\right\} \tag{6}$$

After eliminating the terms containing $\Delta T(x,t)$, the following integral term is left.

$$\Delta s(q)=\int_0^{t_f} -\lambda(0,t)\Delta q dt \tag{7}$$

since $q(t)\in L_2(0,t_f)$, one can write:

$$\Delta s(q)=\int_0^{t_f} \Delta q \nabla s[q(t)]dt \tag{8}$$

Comparing the last two equations, one obtains

$$\nabla s[q(t)]=-\lambda(0,t) \tag{9}$$

Eq. (9) is used to calculate the objective function gradient. Note that in the adjoint problem the last condition is the value of $\lambda(x,t)$ at $t = t_f$. However, the final value problem Eqs. (6) can be transformed into an initial value problem by defining a new time variable given by $\tau = t_f - t$.

5. The conjugate gradient algorithm (CGM)

The unknown function $q(t)$ can be determined by a procedure based on minimizing of the objective function $s[q(t)]$ with an iterative approach by a proper selection of the direction of descent and the search step size. The following iterative scheme is considered as conjugate gradient method (CGM) to estimate the unknown heat flux[20]

$$q^{k+1}(t) = q^k(t) - \beta^k d^k(t) \tag{10}$$

where k denotes the iteration number. The direction of descent $d^k(t)$ is approximated from the following formula

$$\left.\begin{aligned} d^k(t) &= -\nabla s[q^k(t)], \quad for\ k = 0 \\ d^k(t) &= -\nabla s[q^k(t)] + \gamma^k d^{k-1}(t), \ for\ other\ k \end{aligned}\right\} \tag{11}$$

The conjugate coefficient is defined according to the following expression

$$\left.\begin{aligned} \gamma^0 &= 0 \\ \gamma^k &= \frac{\int_0^{t_f} \left\{\nabla s[q^k(t)] - \nabla s[q^{k-1}(t)]\right\} \nabla s[q^k(t)]dt}{\int_0^{t_f} \left\{\nabla s[q^{k-1}(t)]^2\right\} dt} \end{aligned}\right\} \tag{12}$$

To implement the iterative procedure, one needs to develop expression for the optimal search step size β^k and solve the sensitivity problem by setting $\Delta q(t) = d^k(t)$. The following formula is used for the calculation of β^k

$$\beta^k = \frac{\int_0^{t_f} [T(x_{sd}, t; q^k(t)) - T_f] \Delta T(x_{sd}, t; d^k(t))dt}{\int_0^{t_f} [\Delta T(x_{sd}, t; d^k(t))]^2 dt} \tag{13}$$

The following stopping criterion is chosen to stop the iterative procedure

$$s[q^{k+1}(t)] < \varepsilon \tag{14}$$

where ε is the specified tolerance of the order -6 for the noise free data and will be computed using discrepancy principle for noisy data.

6. Simulation and results

A second order central space finite difference and a third order compact Runge-Kutta scheme, RK3, is considered for computing the spatial derivative and the time advancement in direct, sensitivity and adjoint equations, respectively. The time advancement scheme developed by Wray [21] is used for the time marching of the simulation. According to this scheme, the time advancement is performed in three sub-steps. Detailed discussions along with some numerical tests to evaluate the order of accuracy of the numerical approach can be found in reference [21].

The aforementioned inverse method is applied for a material with *Ste* = 1.5. To validate the method, consider that the liquid is initially at $T_i = 0.5$.

A known heat flux is exposed to the boundary and the calculated temperature at sensor location is used as temperature measurement. A triangular heat flux with the following equation is applied for time $t_f = 0.3$.

$$q(t) = \begin{cases} 120t + 15, & 0 \le t < 0.125 \\ -120t + 45, & 0.125 \le t < 0.25 \\ 15, & t \ge 0.25 \end{cases} \tag{15}$$

The exact and computed heat flux (triangular) and resulting interface locations are illustrated in Figs. 2 and 3. The accuracy of heat flux reconstruction is weaker when the sensor is far from the active boundary as illustrated in Fig. 2.

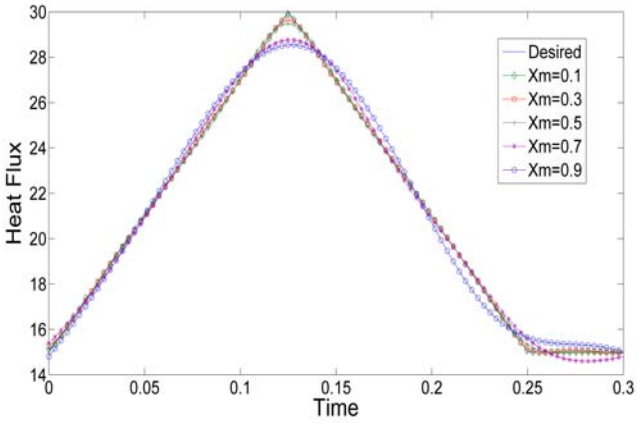

Fig. 2 Desired and reconstructed triangular heat flux for different sensor locations

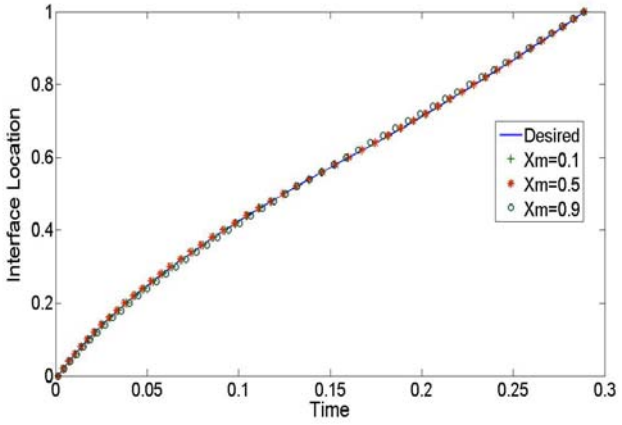

Fig. 3 Desired and computed interface locations for triangular heat flux

Although the reconstructed heat flux has weak accuracy, it shows a good estimation for the interface location. The reduction rate of the objective function is shown in Fig. 4. It indicates the convergence rate of the numerical solution.

To evaluate the performance of the numerical ap-

proach in problems with sharp gradients, the following step function is applied as an input and recovered by the inverse approach.

$$q(t)=\begin{cases}10, & 0\le t<0.15\\ 20, & 0.15\le t<0.3\end{cases} \tag{16}$$

The desired and computed heat flux for different sensor locations is depicted in Fig. 5. Also, Fig. 6 shows the reduction rate of the objective function for the step function.

From the obtained results, it is clear that the method have a good convergence and acceptable results even when the sensor is far away from the active boundary for different types of heat flux containing sharp gradient in the step function.

In order to evaluate the difference between the desired and estimated heat flux, a relative root mean square error e_{RMS} is defined as

$$e_{RMS}=\frac{\sqrt{(1/M)\sum_{m=1}^{M}(q_{desired,m}-q_{estimate,m})^2}}{\sqrt{(1/M)\sum_{m=1}^{M}(q_{desired,m})^2}}\times 100 \tag{17}$$

where M is the total number of time steps. The comparison of the error estimation is illustrated in Fig. 7 for different sensor locations. It can be seen that although all sensor locations have acceptable range of error, the error increases gradually as the sensor becomes far from the boundary. Thus in inverse heat flux estimation the sensor must be as closely as possible to the active boundary. This phenomenon will have a special importance in controlling the solidification interface velocity because in such a kind of problem there is a moving sensor exactly located at the interface and it goes far from the active boundary gradually. Then it is expected that the solidification control results become less accurate in comparison with the stationary sensor locations.

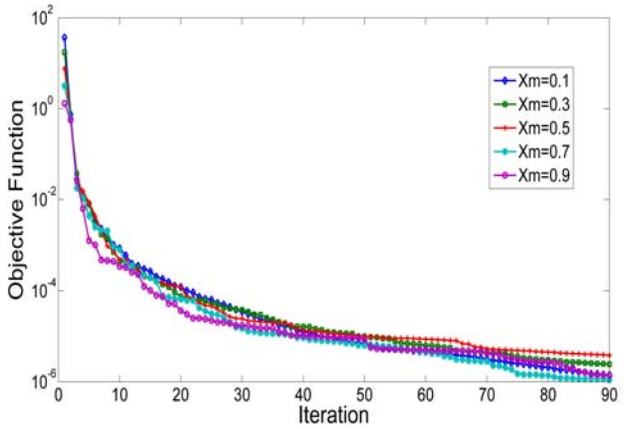

Fig. 4 Objective function reduction rate for triangular heat flux

The proposed approach is tested over a range of Stefan numbers and it is observed that the method is independent of the Stefan number. A quantitative representation of the effect of Stefan number, the RMS error for a wide range of Stefan number at different sensor locations is presented in Table 1 for step heat flux. It is obvious that the Stefan number does not have an important effect on the solution of inverse problem using the proposed approach especially for the heat flux with sharp gradient.

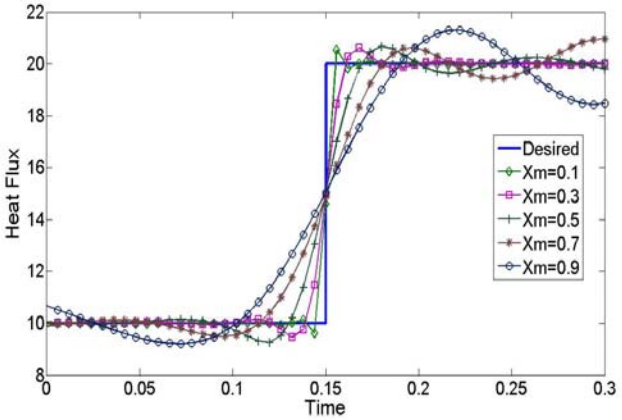

Fig. 5 Desired and reconstructed step heat flux for different sensor locations

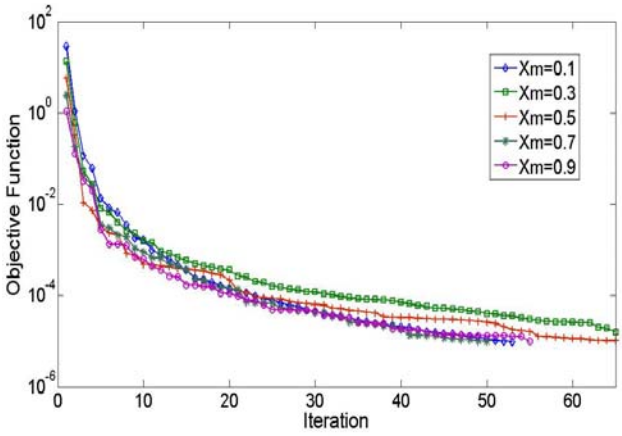

Fig. 6 Objective function reduction rate for step heat flux

7. Effect of measurement errors

In order to evaluate the effectiveness and stability of the inverse method under noisy data, a random noise is added to the measured data. This is of the great importance for practical applications because there are some noises in measured data due to the measuring device errors. The simulated measurement data are constructed by perturbing the exact temperature T^{ex} which obtained from the test heat flux simulation, with an artificial measurement error ω using the following formula

$$T(X_m)=T^{ex}+\sigma\omega \tag{18}$$

where σ is the standard deviation of the measurement and ω is generated from a zero mean normal distribution with variance one. In this study different values of σ are chosen to evaluate the stability of the method under the real practical conditions.

The stopping criterion in equation (14) is modified using the following discrepancy principle for the perturbed data

$$\varepsilon=\sigma^2 t_f \tag{19}$$

Table 1

Comparison of RMS of computed heat flux for different Stefan numbers

	RMS Error (%)				
Stefan Number	$X_m = 0.1$	$X_m = 0.3$	$X_m = 0.5$	$X_m = 0.7$	$X_m = 0.9$
0.5	2.33	4.39	6.14	8.05	10.15
1	2.37	4.37	6.52	8.82	10.22
1.5	2.32	4.39	6.14	8.05	10.16
2	2.32	4.44	7.83	9.14	10.56

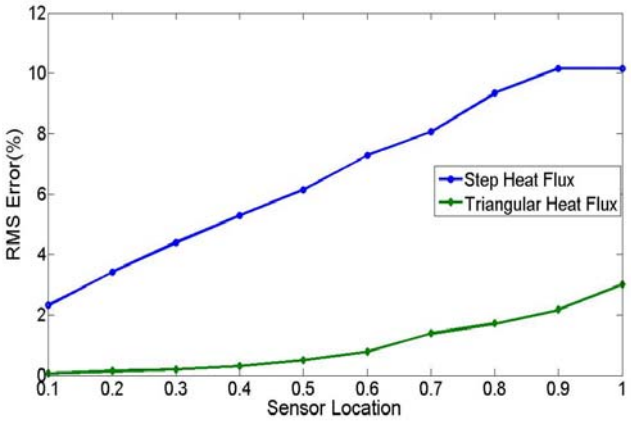

Fig. 7 Heat flux RMS error estimation for different sensor locations

Different measurement errors with different standard deviations are considered at $X_m = 0.1$. Other sensor locations are not considered due to the fact that sensors which are far from the active boundary make the solution less accurate. Thus the sensors at the start and the middle point of the mould are investigated. The reconstructed heat flux for noisy and noise free measurements for $X_m = 0.1$ is shown in Fig. 8 and 9 for triangular and step shape heat fluxes, respectively. Table 2 shows the values of RMS error of estimation and the final value of objective function for different noise values. As indicated, the obtained results are still acceptable even with noisy data of $\sigma = 0.1$. However, due to strong ill-posed of the considered inverse problem, the accuracy of the solution becomes weaker and the estimation results could be unreliable with larger noisy data employed.

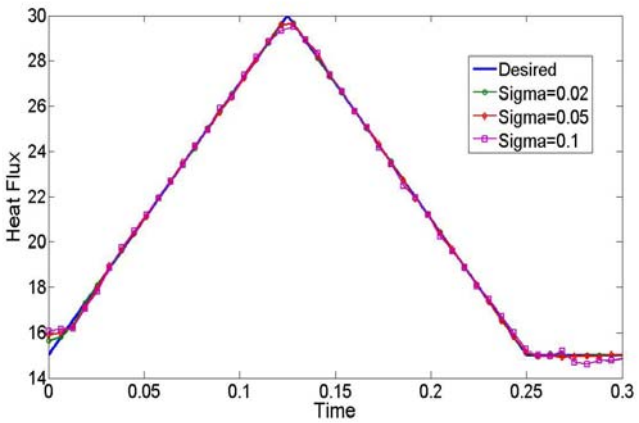

Fig. 8 Reconstructed triangular heat flux of noisy measured temperature at $X_m = 0.1$

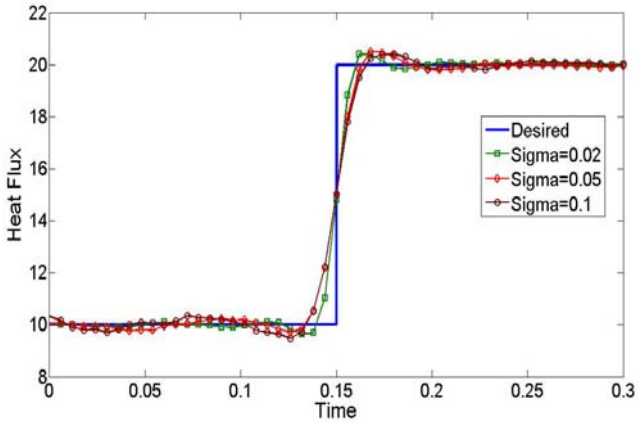

Fig. 9 Reconstructed step heat flux of noisy measured temperature at $X_m = 0.1$

Table 2

Comparison of objective function and RMS of computed heat flux for different σ

Triangular Heat Flux		
σ	Objective Function	RMS Error (%)
0	9.88E-07	0.056
0.02	2.28E-04	0.363
0.05	1.3E-03	0.58
0.1	4.9E-03	0.62

Step heat flux		
σ	Objective Function	RMS Error (%)
0	9.65E-06	2.32
0.02	2.20E-04	2.70
0.05	1.3E-03	3.32
0.1	5E-03	3.62

8. Conclusion

A transient inverse solidification problem was formulated and solved by applying the conjugate gradient optimization method. In addition, the enthalpy formulation was applied to solve the inverse problem in a fixed domain to avoid the solution for liquid and solid phases separately. Two known heat flux test cases were considered as boundary condition to generate the time history of temperatures at sensor locations. These temperatures were used to reconstruct the boundary heat flux. The obtained results indicated that the accuracy and the convergence of the solution become stronger when the sensor is located near to active

boundary. To evaluate the performance of the method to random noise in measured data, a random noise with $\sigma = 0.02, 0.5$ and 0.1 was added into the measured temperatures. The reconstructed heat fluxes indicated a weak dependency on noisy data even for large relative noises. It was shown that the stability and accuracy of the estimation become weak with large noise amplitudes due to ill-posed of the inverse heat transfer problems.

References

1. **Beck, J.V., Blackwell, B., Clair, C.** Inverse Heat Conduction: ill Posed Problems. -New York: John Wiley & Sons, 1985.-308p.
2. **Flemings, M.C.** Solidification Processing. -New York: McGraw-Hill, 1974.-364p.
3. **Voller, V.R.** Enthalpy method for inverse Stefan problems, -Numer. Heat Trans. Part B: Fundam. 1992, v.21, No.1, p.41-55.
4. **Kang, S., Zabaras, N.** Control of the freezing interface motion in two-dimensional solidification processes using the adjoint method, -Int. J. Numer Methods Eng., 1995, v.38, p.63-80.
5. **Sampath, R., Zabaras, N.** Adjoint variable method for the thermal design of eutectic directional solidification processes in an open-boat configuration, -Numer. Heat Trans., 2001, v.39, p.655-683.
6. **Yang, G.Z., Zabaras, N.** The Adjoint Method for an Inverse Design Problem in the Directional Solidification of Binary Alloys, -J. Comput. Phys., 1998, v.140, No.2, p.432-452.
7. **Yang, G.Z., Zabaras, N.** An adjoint method for the inverse design of solidification processes with natural convection, Int. -J. Numer. Methods Eng., 1998, v.42, p.1121-1144.
8. **Zabaras, N.** Dynamic programming approach to the inverse Stefan design problem, -Numer. Heat Trans., 1994, v.26, p.97-104.
9. **Zabaras, N.** On the design of two-dimensional Stefan processes with desired freezing front motions, -Numer. Heat Trans., 1992, v.21, p.307-325.
10. **Zabaras, N., Enguyen, H.T.** Control of the freezing interface morphology in solidification processes in the presence of natural convection, -Int. J. Numer. Methods Eng., 1995, v.38, p.1555-1578.
11. **Zabaras, N., Mukherjee, S., Richmond, S.** An analysis of inverse heat transfer problems with phase changes using an integral method, -J. Heat Trans., 1988, v.110, p.554-561.
12. **Frankel J.I., Keyhani M.** A new approach for solving inverse solidification design problems, Numer. Heat Trans. Part B: Fundam., 1996, v.30, No.2, p.161-177.
13. **Hale, S.W., Keyhani, M., Frankel, J.I.** Design and control of interfacial temperature gradients in solidification, -Int. J. Heat Mass Trans., 2000, v.43, No.20, p.3795-3810.
14. **Xu, R., Naterer, G.F.** Controlled interface acceleration in unidirectional solidification, -Int. J. Heat Mass Trans., 2004, v.47, No.22, p.4821-4832.
15. **Xu, R., Naterer, G.F.** Deterministic physical influence control of interfacial motion in thermal processing of solidified materials, -Exp. Therm. Fluid Sci., 2005, v.29, No.2, p.227-238.
16. **Xu, R., Naterer, G.F.** Inverse method with heat and entropy transport in solidification processing of materials, -J. Mater. Process. Technol., 2001, v.112, No.1, p.98-108.
17. **Okamoto, K., Li, B.Q.** A regularization method for the inverse design of solidification processes with natural convection, -Int. J. Heat Mass Trans., 2007, v.50, No.21-22, p.4409-4423.
18. **Hinze, M., Ziegenbalg, S.** Optimal control of the free boundary in a two-phase Stefan problem, -J. Comput. Phys., 2007, v.223, No.2, p.657-684.
19. **Hill, J.M., Dewynne, J.N.** Heat Conduction, Blackwell Scientific Publication, -Oxford, 1987.-334p.
20. **Ozisik, M.N., Orlande, H.R.B.** Inverse Heat Transfer, Fundamentals and Applications, Taylor & Francis, -New York, 2000.-330p.
21. **Maghrebi, M.J.** A Study of the Evolution of Intense Focal Structures in Spatially Developing Three-Dimensional Plane Wakes, Ph.D. diss., Monash University, 1999.-198p.

Abbas Nejad, M.J. Maghrebi, H. Basirat Tabrizi

SENSORIAUS PADĖTIES ĮTAKA ATVIRKŠTINĖS STEFANO PROBLEMOS SPRENDIMUI

R e z i u m ė

Šio tyrimo tikslas – įvertinti sensoriaus padėties įtaką sprendžiant atvirkštinę Stefano problemą. Tiesinis laidumas yra panaudotas sukietėjimo procesui valdyti. Entalpijos sąvoka kartu su jungtiniu gradiento metodu yra panaudoti krypties problemoms formuluoti ir tikslo funkcijai minimizuoti. Sensoriaus padėties kvadratinio nukrypimo suma tarp išmatuotos ir apskaičiuotos temperatūros panaudotos kaip tikslo funkcija. Matuojamos temperatūros modeliuojamos naudojant tiesinį trikampio ir slenksčio pavidalo ribinį šilumos srovės sprendinį. Parinktos skirtingos sensoriaus padėtys besiplečiančios erdvės skaičiavimo srityse. Rezultatai rodo, kad esant sensoriui toliau nuo aktyvių ribų (ribų, kuriose veikia šilumos perdavimo srovės) paklaida restauruotoje šilumos erdvėje yra didesnė ir atvirkščiai. Ištyrus įvedimo duomenų trukdžių efektą matyti, kad net esant aukštam matavimo duomenų trukdžių lygiui sprendimas būna stabilus.

A. Abbas Nejad, M.J. Maghrebi, H. Basirat Tabrizi

EFFECT OF SENSOR LOCATIONS ON THE SOLUTION OF INVERSE STEFAN PROBLEMS

S u m m a r y

The aim of this study is to investigate the effect of sensor location on the solution of inverse Stefan problems. A unidirectional conduction driven solidification process is considered. The enthalpy formulation along with conjugate gradient method is used to simulate the direct problem and minimize the objective function. The sum of square deviation between the measured and the calculated temperatures at sensor location is defined as objective function. Measured temperatures are simulated using direct solver for

triangular and step shape boundary heat fluxes. Different sensor locations in the spatial extent of the computational domain are selected. The results show that as the sensor is taken further from the active boundary (the boundary which heat flux applied on it) the error in reconstructed heat flux becomes larger and vice versa. Also the effect of noisy input data is investigated which indicate that the solution is stable even in high noise levels in measured data.

Аббас Неяд, М.Й.Магхреби, Х.Басират Табризи

ВЛИЯНИЕ ПОЛОЖЕНИЯ СЕНСОРА ДЛЯ РЕШЕНИЯ ОБРАТНОЙ ПРОБЛЕМЫ СТЕФАНА

Р е з ю м е

Целью этого исследования является оценка влияния положения сенсора при решении обратной проблемы Стефана. Для управления процессом затвердения использовалась прямая проводимость. Формулировка энтальпии вместе с методом объединенного градиента использовались для решения проблемы направления и минимизации целевой функции. Измеряемые температуры моделировались при использовании линейного треугольного и порогового предельного решения для теплового потока. Подобранные разные положения сенсора в расчетных областях расширяющегося пространства. Результаты расчета показали, что при положении сэнсора дальше от активных пределов (пределов, где действуют потоки передаваемого тепла) ошибка в реставрируемом тепловом пространстве является большей и наоборот. Исследован эффект помех вводимых данных показал, что даже значительные помехи измеряемых данных дают стабильное решение.

Received January 19, 2010
Accepted June 11, 2010